JOURNAL OF MATERIALS SCIENCE 18 (1983) 1645–1649

Heat evolution investigated by a liquid crystal film technique during fracture in metals

AKIRA KOBAYASHI*, HIROSHI SUEMASU†
Faculty of Engineering, Institute of Interdisciplinary Research, University of Tokyo, Komaba-4-Chome-6-1, Meguro-Ku, Tokyo 153, Japan

Heat evolution caused from a running crack front during dynamic fracture in steels, aluminium alloys and titanium alloys was investigated through liquid crystal film visualization, and a correlation between the generated heat and the crack propagation velocity was found. The heat evolution increased with an increase in the crack velocity for an individual metal. The magnitude of heat evolution was largest for steels having the lowest crack velocity, while the titanium alloy produced the smallest heat evolution, but showed the highest crack velocity. In comparison the aluminium alloy gave intermediate values of heat evolution and crack velocity.

1. Introduction

During dynamic crack propagation in solids, high energy concentration at the running crack tip gives rise to a phenomenon in which the heat generated from this running crack tip can be observed as the thermal boundary front movement indicated by the changes in colour through the liquid crystal film technique [1–4]. Already the present authors have investigated this topic with carbon-fibre composites [5] and polymers [6]. Fuller *et al.* [7] have also studied polymers in this respect. In the present report, heat evolution during dynamic crack propagation in metals, i.e. steels, aluminium alloys and titanium alloys, will be presented through the visible liquid crystal film technique.

2. Experimental procedures

2.1. Loading apparatus

The experiment was performed under mode I crack propagation conditions at room temperature, and the applied crosshead speeds were 100 and 500 mm min^{-1}. An Instron-type tensile tester UTM-1 of Toyo-Baldwin make was employed. The applied load was measured by a load cell and stored in a transient memory, and simultaneously monitored on an oscilloscope during the test.

2.2. Specimens

The test specimens were prepared for steel SAE 4130, aluminium alloy 2024-T3 and titanium alloy Ti–6Al–4V, the size of which is shown in Fig. 1.

2.3. Velocity gauges

Du-Pont conductive silver coating material no. 4817, the conducting wires in short, were placed at certain intervals on the projected path of the crack, and perpendicular to the direction of crack propagation as shown in Fig. 1. These wires formed one leg of a bridge in the electronic circuit, connected to a transient memory. Since the metal specimens are electrically conductive, a thin epoxy layer was first applied to the specimen surface and then the velocity gauges were applied. The time at which these wires broke owing to the running crack was obtained afterwards from the trace on the pen recorder. Thus the average crack propagation velocity between the wires could be obtained

*Professor.
†Research Fellow.

0022–2461/83 $03.00 + .12

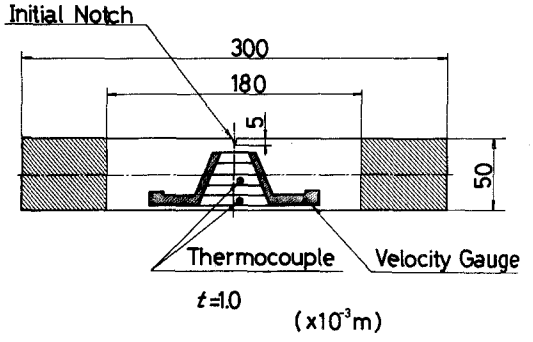

Figure 1 Specimen configuration with the velocity gauge and thermocouples (liquid crystal film is on the reverse side).

from the wire interval and the time required for a crack to pass between the wires. The electrical signal due to the wire breaking was stored in a transient memory, which was reproduced afterwards on the pen recorder, and was also monitored on an oscilloscope. For further details see Kobayashi *et al.* [8].

2.4. Thermocouples

Copper–constantan thermocouples with 0.1 mm diameter were attached at two locations on the specimen surface as shown in Fig. 1. The output obtained was recorded by the pen recorder.

2.5. Liquid crystal film

As is known, liquid crystal film is optically anisotropic and has a colour sensitivity to changes in temperature [9].

A thin liquid crystal layer, about 100 μm thick, was spread over the specimen surface painted matt black, on the surface opposite to the velocity gauge side, across the surface where the crack advance was anticipated. The liquid crystal used was a mixture of about 50 wt% cholesteryl oleyl carbonate and 50 wt% cholesteryl nonanoate, changing from colourless to red at 29.05° C and from green to blue at 29.70° C as shown in Fig. 2. As shown in Fig. 3, a video camera system was used to take colour photographs of moving thermal boundary fronts emanating from the running crack front observed on the liquid crystal film. The video camera was operated by a trigger gauge as soon as the crack propagation started.

2.6. Block diagram

The block diagram of measurement is shown in Fig. 3.

3. Calculation of heat evolution

The heat evolved at the running crack tip can be estimated from the thermal boundary fronts obtained by the changes in colour through liquid crystal film visualization, by using several assumptions as stated below.

1. One-dimensional heat flow.
2. No heat loss from the specimen surface.
3. The specimen length is infinite.
4. The heat origin is very small with no volume.
5. The crack propagation velocity, $\dot{C}$, is far greater compared with the heat conduction velocity.
6. The colour thermal boundary fronts obtained are isothermal: T_1 is blue/green at 29.70° C, and T_2 is colourless/red at 29.05° C (Fig. 4).
7. $(Q_1 - Q_2)^2$ be minimized, where Q_1 is the heat evolution at $y = y_1$ and Q_2 is the heat evolution at $y = y_2$, as indicated in Fig. 4.

From the conventional heat conduction equation [10] we have

$$Q = \rho c(4\pi kt)^{1/2}\Delta T\, e^{y^2/4kt} \qquad (1)$$

with the associated coordinates shown in Fig. 4, where Q is the heat evolved on both crack faces per unit area of crack advance, k is the thermal diffusivity $= K/\rho c$, K is thermal conductivity, c the specific heat, ρ the density, t the time elapsed after fracture, T is the temperature, and y is the distance from the cracked plane.

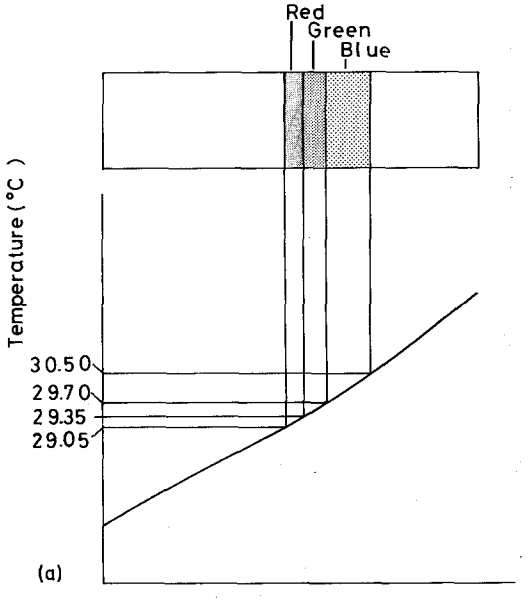

Figure 2 (a) Colour sensitivity to changes of temperature in liquid crystal film. (b) The attached colour picture is for steel subjected to a crosshead speed of 500 mm min^{-1} for 20 sec after fracture.

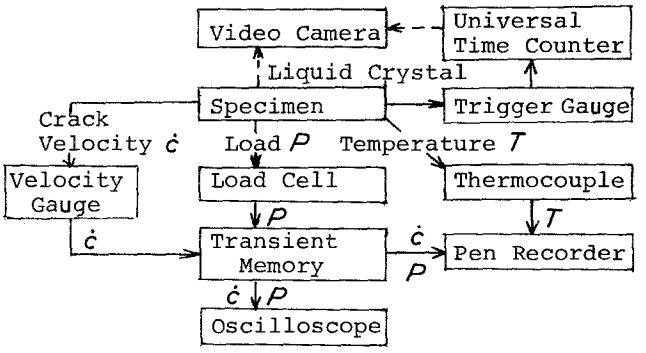

Figure 3 Block diagram of measurement.

We have the following equation to calculate the heat evolution obtained from the liquid crystal film visualization technique:

$$Q = \rho c(4\pi kt)^{1/2} e^{y_1^2/4kt} \times \frac{\int_0^b e^{y_2^2/4kt}(e^{y_2^2/4kt} - e^{y_1^2/4kt})\,dx}{\int_0^b (e^{y_2^2/4kt} - e^{y_1^2/4kt})^2\,dx} \Delta T \quad (2)$$

where $b\,(= 50\,\text{mm})$ is the specimen width, and k is obtained from K, c and ρ given in Table I.

4. Experimental results and discussions

In the present experiment, the 4130 steels and the 2024-T3 aluminium alloys were both tested under mode I crack propagation loading in tension subject to both 100 and 500 mm min^{-1}, while only 500 mm min^{-1} tension loading in mode I propagation was applied to the Ti–6Al–4V alloys. In calculating the crack propagation velocity, $\dot{C}$, the velocity gauge values were calibrated by the video camera recording data for the steel specimen case, since the steel specimens showed very ductile breaking so that the velocity gauges could not show a sharp signal on the electronic recording data.

For the heat evolution calculation, the heat evolution Q was calculated from Equation 2, as described previously, by using the thermal boundary fronts, T_1 and T_2, which were observed through liquid crystal film visualization.

Among the load against displacement curves monitored during loading, those for the titanium alloys showed a typical brittle load against displacement curves, although no curves presented here.

Figs. 5 to 7 show the heat evolution Q and the crack propagation velocity, $\dot{C}$, as a function of a running crack front position, C/C_0, where C is the arbitrary crack length, and $C_0\,(= 5\,\text{mm})$ is the initial crack length. In view of the experimental results shown in Figs. 5 to 7, the heat increases

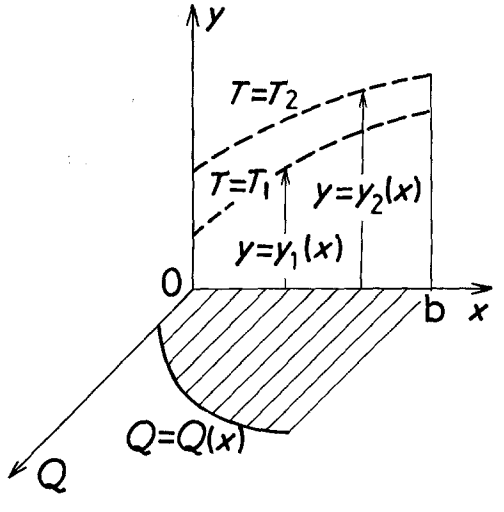

Figure 4 Coordinates and heat evolution.

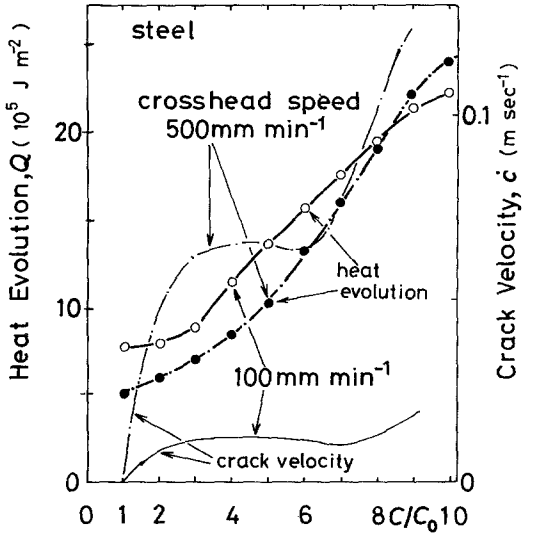

Figure 5 Heat evolution and crack velocity (steel).

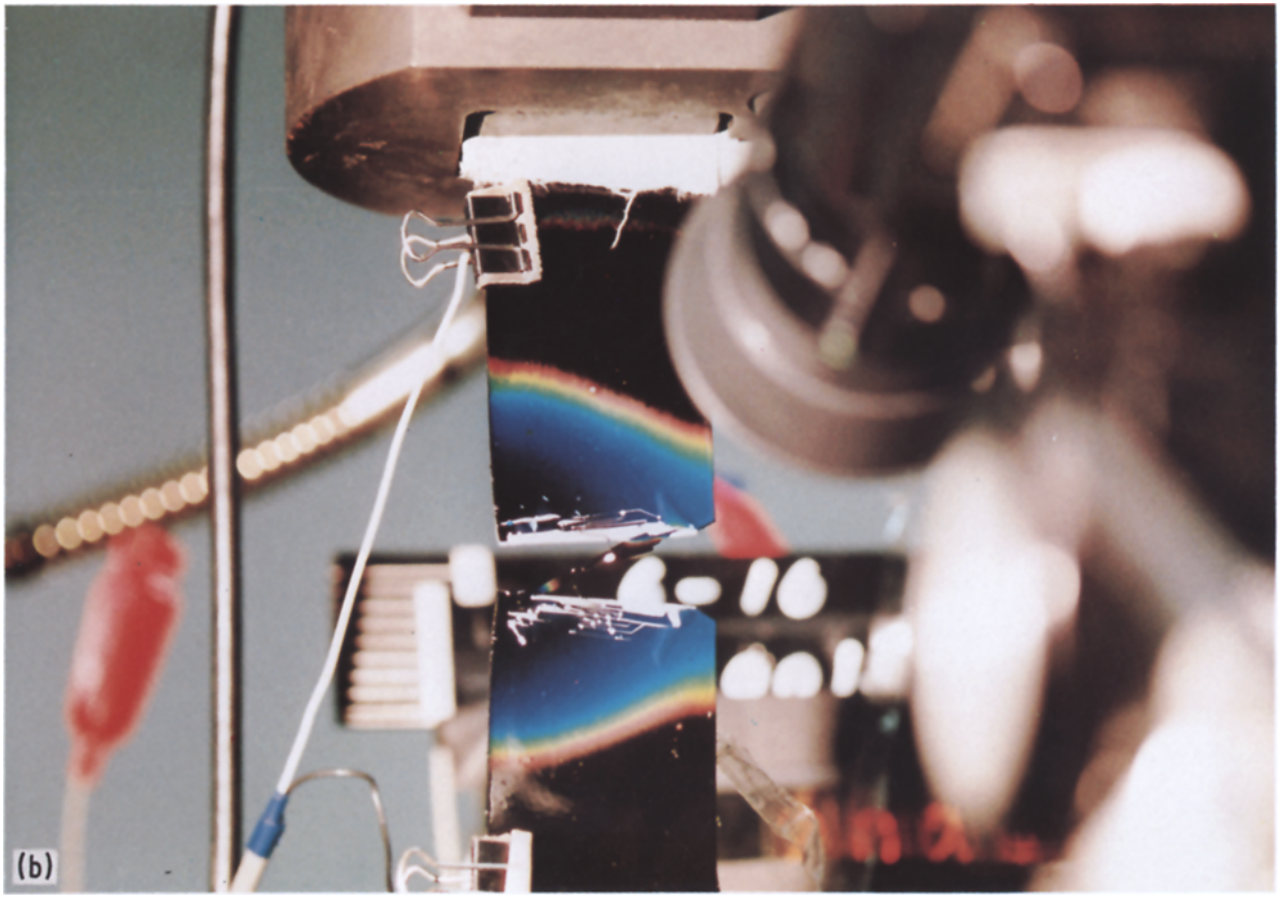

Figure 2 Continued.

TABLE I Physical properties of metals

	Specific heat, c ($\times 10^2$ J kg^{-1} °C^{-1})	Thermal conductivity, K (J m^{-1} sec^{-1} °C^{-1})	Density, ρ ($\times 10^3$ kg m^{-3})	Young's modulus, E (GN m^{-2})
Aluminium alloy 2024-T3	9.6	120	2.8	70
Titanium alloy Ti–6Al–4V	5.0	6.7	4.7	120
Steel	4.6	52	7.8	210

with the increase in the crack velocity for all cases, though there exist some wavy crack velocity profiles especially for steels and aluminium alloys. The magnitude of heat evolution is, roughly speaking, rather an inversely increasing function of the crack propagation velocity, in comparison with these three metals. That is, the steel shows the largest heat evolution, while its crack velocity is the lowest. The titanium alloy produces the highest crack velocity but has the smallest heat evolution. The aluminium alloy gave intermediate values of both heat and crack velocity.

The crosshead speed effects on the heat evolution are hardly observed for both the steel and the aluminium alloy cases, far from that, the apparent inversion is even observed in the steel case: greater heat evolution can be obtained almost all the way for the 100 mm min^{-1} case, as seen in Fig. 5.

The heat evolution, Q, plotted against crack propagation velocity, $\dot{C}$, is summarized in Fig. 8 and gives a comparison of the three metals tested.

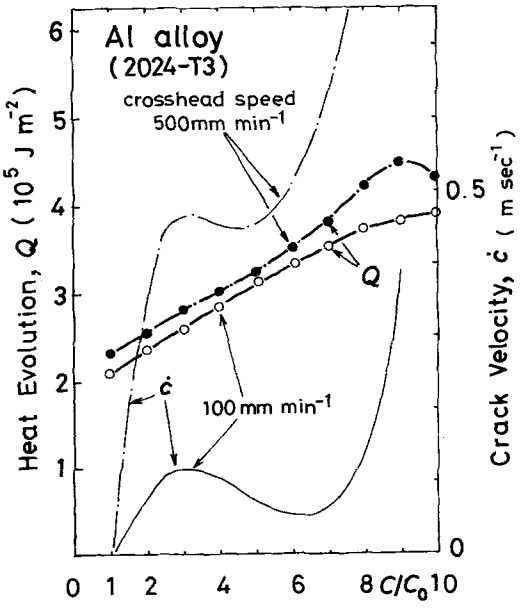

Figure 6 Heat evolution and crack velocity (aluminium alloy).

The temperature rise was obtained from the thermocouple recording, and the heat evolution could also be calculated from the following equation:

$$Q = \rho c \frac{\int_0^{t_{max}} T_0(t)/(4\pi kt)^{1/2}\, e^{(-y^2/4kt)}\, dt}{\int_0^{t_{max}} 1/(4\pi kt)\, e^{(-y^2/2kt)}\, dt} \quad (3)$$

where T_0 is the temperature measured by the thermocouples.

Using this heat evolution the theoretical temperature profile can be obtained. We can then compare this calculated temperature profile with the experimental temperature profile measured by the thermocouple. Such a comparison is shown in Fig. 9 and the two profiles show good agreement.

5. Conclusions

The heat evolved emanating from a running crack front in steels, aluminium alloys and titanium alloys has been experimentally calculated using

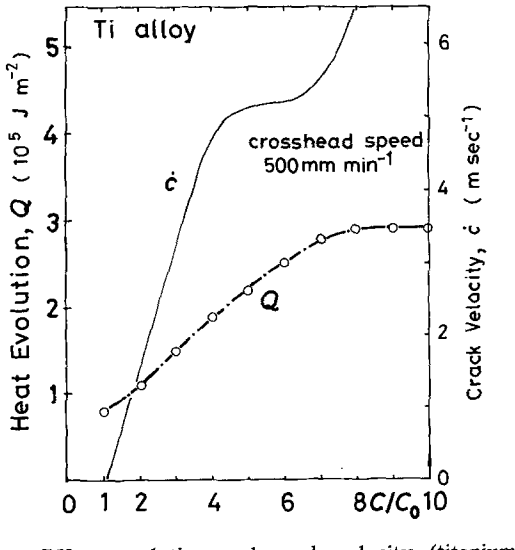

Figure 7 Heat evolution and crack velocity (titanium alloy).

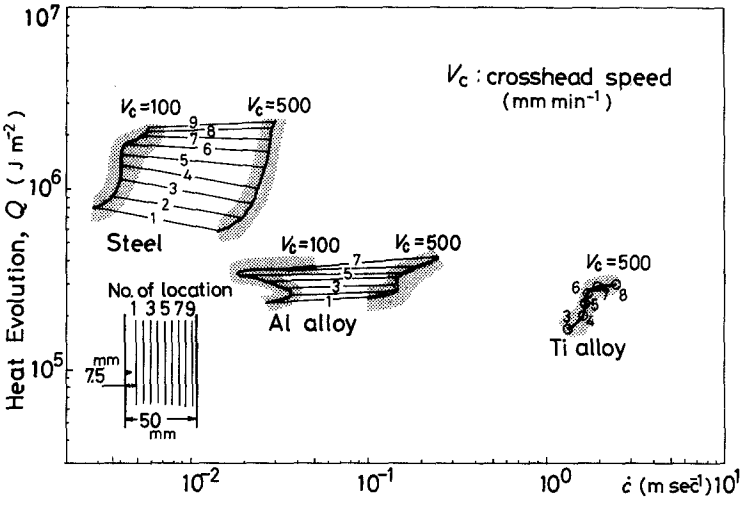

Figure 8 Heat evolution and crack velocity (comparison of the steel, aluminium alloy and titanium alloy).

appropriate assumptions and by observing the thermal boundary front as the coloured isothermal front through liquid crystal film visualization. It was found that heat evolution increased with the increase in the crack propagation velocity, in general, for the individual metal case. The magnitude of heat evolution is greatest for steel and smallest for the titanium alloy, while the aluminium alloy gives an intermediate value. The magnitude of the crack propagation velocities obtained for the three metals is in the reverse order of that for heat evolution.

Acknowledgements

The authors wish to express their appreciation to Mr Masayuki Munemura, Mr. Takashi Kurita, and Mr Akira Hoshi for their assistance with the present research. Mitsubishi Heavy Industries are acknowledged for offering the test materials. This work is partially supported by Keikinzoku Shogakkai, Japan.

References

1. R. WEICHERT and K. SCHONERT, *J. Mech. Phys. Solids* **26** (1978) 151.
2. A. KOBAYASHI and N. OHTANI, *Rep. Inst. Space Aeronaut Sci. Univ. Tokyo* No. 529 (1975).
3. R. ATTERMO and G. OSTBERG, *Int. J. Fract. Mech.* **7** (1971) 122.
4. W. DOLL, *Eng. Fract. Mech.* **5** (1973) 259.
5. A. KOBAYASHI and H. SUEMASU, in Proceedings of the First Japan–US Conference on Composite Materials, Tokyo, January 1981 (Japan Society for Composite Materials, Tokyo, 1981) p. 339.
6. A. KOBAYASHI, M. MUNEMURA, N. OHTANI and H. SUEMASU, *Bull. Inst. Space Aeronaut Sci. Univ. Tokyo* **17** 1(B) (1981) 459.
7. K. N. G. FULLER, P. G. FOX and J. E. FIELD, *Proc. Roy. Soc. London A* (1975) 341, 537.
8. A. KOBAYASHI, N. OHTANI and T. SATO, *J. Appl. Polym. Sci.* **18** (1974) 1625.
9. J. L. FERGASON, *Appl. Opt.* **7** (1968) 1729.
10. H. S. CARSLAW and J. C. JAEGER, "Conduction of Heat in Solids" (Oxford University Press, Oxford, 1959) p. 259.

Received 16 September
and accepted 21 October 1982

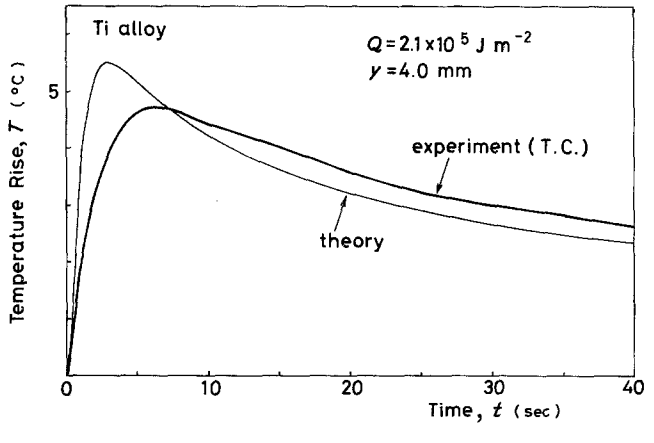

Figure 9 Comparison of temperature rise (titanium alloy).